Neuropsychopharmacology (2014) 39, 3100–3111

www.neuropsychopharmacology.org

Reduced Phenotypic Severity Following Adeno-Associated Virus-Mediated Fmr1 Gene Delivery in Fragile X Mice

Shervin Gholizadeh[1,3], Jason Arsenault[1,3], Ingrid Cong Yang Xuan[1], Laura K Pacey[1] and David R Hampson*[,1,2]

[1]Department of Pharmaceutical Sciences, Leslie Dan Faculty of Pharmacy, University of Toronto, Toronto, ON, Canada; [2]Department of Pharmacology, Faculty of Medicine, University of Toronto, Toronto, ON, Canada

Fragile X syndrome (FXS) is a neurodevelopmental disorder caused by a trinucleotide repeat expansion in the FMR1 gene that codes for fragile X mental retardation protein (FMRP). To determine if FMRP expression in the central nervous system could reverse phenotypic deficits in the Fmr1 knockout (KO) mouse model of FXS, we used a single-stranded adeno-associated viral (AAV) vector with viral capsids from serotype 9 that contained a major isoform of FMRP. FMRP transgene expression was driven by the neuron-selective synapsin-1 promoter. The vector was delivered to the brain via a single bilateral intracerebroventricular injection into neonatal Fmr1 KO mice and transgene expression and behavioral assessments were conducted 22–26 or 50–56 days post injection. Western blotting and immunocytochemical analyses of AAV–FMRP-injected mice revealed FMRP expression in the striatum, hippocampus, retrosplenial cortex, and cingulate cortex. Cellular expression was selective for neurons and reached ~50% of wild-type levels in the hippocampus and cortex at 56 days post injection. The pathologically elevated repetitive behavior and the deficit in social dominance behavior seen in phosphate-buffered saline-injected Fmr1 KO mice were reversed in AAV–FMRP-injected mice. These results provide the first proof of principle that gene therapy can correct specific behavioral abnormalities in the mouse model of FXS.
Neuropsychopharmacology (2014) **39,** 3100–3111; doi:10.1038/npp.2014.167; published online 6 August 2014

INTRODUCTION

Fragile X syndrome (FXS), caused by a pathological CGG trinucleotide extension in the 5′ untranslated region of the FMR1 gene, is the most prevalent single-gene disorder linked to mental retardation and autism spectrum disorders (Bagni *et al*, 2012). The CGG repeat range in unaffected individuals is 5–55, whereas expansions of 200 or more result in gene hypermethylation and FXS. The highly expanded CGG repeat also causes the transcribed mRNA to form RNA–DNA heteroduplexes (Colak *et al*, 2014), which together with gene hypermethylation severely reduces or abrogates the expression of Fragile X Mental Retardation Protein (FMRP). Trinucleotide expansions in the intermediate range of 70–199 repeats results in the formation of toxic intranuclear inclusions, a mild reduction of FMRP, and are associated with the neurodegenerative disorder Fragile X-associated Tremor and Ataxia syndrome (Bagni *et al*, 2012; LaFauci *et al*, 2013; Ludwig *et al*, 2014). Reduced FMRP expression has also been reported in other mental disorders including autism, schizophrenia, bipolar disorder, and major depression (Fatemi and Folsom, 2011).

FMRP is an mRNA binding protein that controls translation of its bound mRNA substrates. More than 800 different identified gene transcripts have been shown to bind to FMRP in mouse brain tissue and in human cell lines (Ascano *et al*, 2012; Darnell *et al*, 2011). In the CNS, FMRP acts as a transport molecule in neurons to shuttle bound mRNAs to dendrites and synaptic spines where the bound mRNA cargoes are then released and translated. Numerous studies have demonstrated altered synaptic plasticity in animal models of the disorder. For example, studies in mice lacking FMRP revealed altered ocular dominance plasticity in visual cortex and a delayed critical period of synaptic plasticity in barrel cortex (Dölen *et al*, 2007; Harlow *et al*, 2010). Hypersensitivity to auditory stimuli in humans with FXS and mice lacking FMRP suggests that development and plasticity in the auditory system may also be affected by the loss of FMRP (Chen and Toth, 2001; Kim *et al*, 2013a).

Persons with FXS experience a wide range of symptoms including cognitive deficits, social anxiety, attention deficit and hyperactivity disorder, repetitive stereotyped behaviors, seizures, and sensory hypersensitivity (Wijetunge *et al*, 2013). Parallel to human FXS, Fmr1 knockout (KO) mice also display deficits consistent with an 'autistic phenotype'. Fmr1 KO mice display altered synaptic plasticity, hyperactivity, reduced ultrasonic vocalizations during courtship, increased repetitive/stereotypic behaviors, audiogenic

*Correspondence: Dr DR Hampson, Department of Pharmaceutical Sciences, Leslie Dan Faculty of Pharmacy, University of Toronto, 144 College Street, Toronto, ON, Canada M5S3M2, Tel: +1 416 978 4494, Fax: +1 416 978 8511, E-mail: d.hampson@utoronto.ca
[3]These authors contributed equally to this work.
Received 16 April 2014; revised 6 June 2014; accepted 24 June 2014; accepted article preview online 7 July 2014

seizures, and reduced social interactions (Pacey *et al*, 2011a; Pacey *et al*, 2011b; Thomas *et al*, 2011). Thus, Fmr1 KO mice are generally considered as a good animal model of the disorder and are widely used for testing phenotypic reversal after treatment with small molecule drug candidates.

There is no pharmacological cure for FXS and the currently prescribed medications, such as anti-psychotics, antidepressants, and stimulants, only partially alleviate selected symptoms and are associated with deleterious side effects. Newer second generation drugs to treat FXS, including metabotropic glutamate receptor 5 (mGluR5) antagonists, are being investigated in clinical trials (Castren *et al*, 2012; Hampson *et al*, 2012; Pop *et al*, 2014). However, considering the plethora of genes whose expression is regulated by FMRP, *a priori*, it may be expected that restoring FMRP expression in the CNS could provide a more comprehensive reversal of the disorder compared with targeting single molecules (eg, mGluR5). The possibility of restoring normal brain function after introduction of exogenous FMRP into the brain has previously been attempted. Using an adeno-associated virus (AAV)-based vector coding for FMRP, Zeier *et al* (2009) reported that injections directly into the hippocampus of 5-week-old Fmr1 mice resulted in correction of the abnormally enhanced hippocampal long-term synaptic depression (Zeier *et al*, 2009); however, no other analyses of phenotypic rescue were carried out and immunocytochemical analysis showed localized transgene expression only in the hippocampus.

The objective of the present study was to investigate the possibility of developing a more long-term curative therapy for FXS by assessing the efficacy of administering an AAV vector coding for FMRP (AAV–FMRP) directly into the CNS of Fmr1 KO mice via intracerebroventricular (i.c.v.) administration to postnatal day (PND) 5 mice. Previous work reported by our laboratory (Gholizadeh *et al*, 2013) and others (Gray, 2012; Kim *et al*, 2013b; Miyake *et al*, 2011) using AAV vectors coding for green fluorescent protein indicated the utility of i.c.v. administration for achieving more widespread vector diffusion in the brain. Here, we demonstrate that i.c.v. delivery of AAV–FMRP into mouse neonates resulted in protracted FMRP expression in neurons of the cortex, hippocampus, and striatum. Behavioral analysis indicated that administration of AAV–FMRP caused a significant reduction in stereotypic behavior as well as a reversal of deficient social dominance behavior seen in saline-injected Fmr1 KO mice. These findings delineate a first step towards developing a biological therapeutic strategy for correcting the behavioral deficits in FXS.

MATERIALS AND METHODS

Animals and AAV Vectors

All experiments were carried out using C57/BL6J wild-type mice and Fmr1 KO mice backcrossed 10 generations on C57/BL6J mice. All procedures were approved by the University of Toronto Animal Care Committee and were carried out in compliance with the Canadian Council on Animal Care guidelines. A single-stranded AAV vector containing the inverted terminal repeat (ITR) DNA sequences from the genome of AAV2, the capsid protein genes from AAV9, and the human synapsin-1 (SYN) promoter upstream of the mouse coding region (isoform 1) was supplied by the University of Pennsylvania Vector Core Facility (Philadelphia, PA; Figure 1a). This AAV9 vector (AAV–FMRP) was purified and used at a concentration of 1×10^{13} genomes/ml in sterile phosphate-buffered saline (PBS) and stored at $-80\,^{\circ}$C.

Vector Injections

A single bilateral i.c.v. injection of PBS or AAV–FMRP was administered to PND 5 Fmr1 KO mice as described previously (Gholizadeh *et al*, 2013). A group of wild-type mice injected with PBS served as a control group. The pups were immobilized via cryo-anesthesia for 2 min and then grasped by the skin behind the head and placed over a fiber-optic light to illuminate the midline and transverse sutures that were used as a guide for injections. A 30-gauge needle attached to a 5 μl Hamilton syringe (Hamilton, Reno, NV) through long polyethylene tubing was used for injections. The needle was inserted 2 mm deep, perpendicular to the skull surface, at a location ~0.25 mm lateral to the sagittal suture and 0.50–0.75 mm rostral to the neonatal coronary suture. A quantity of 1 μl of the vector or PBS was injected using a syringe pump at the rate of 1 μl/min into each lateral ventricle. The needle was left in place for 1 min after injection after which the needle was slowly retracted to prevent backflow.

Immunocytochemistry and Confocal Microscopy

At 26–30 or 54–56 days post injection, both AAV–FMRP vector-injected and PBS-injected control mice were anesthetized with ketamine and xylazine and perfused transcardially with a solution of PBS followed by 4% paraformaldehyde (pH = 7.4). Serial coronal or sagittal sectioning was performed at a thickness of 25 μm using a cryostat (Leica Microsystems, Wetzlar, Germany). Free-floating sections were rinsed with Tris-buffered saline and antigen retrieval was performed as described previously (Gabel *et al*, 2004). Monoclonal mouse anti-FMRP (2F5; 1 : 1000; gift from Dr Jennifer Darnell) was used along with each of the following monoclonal rabbit primary antibodies: NeuN (1 : 1000; Abcam) to immunolabel neurons and anti-S100β (1 : 1000; Abcam) to mark astrocytes. After overnight incubation, five washes with TBS for 10 min each were carried out and secondary antibodies diluted in TBS containing 5% goat serum were applied. The sections incubated with anti-FMRP were labeled with goat anti-mouse Alexa Fluor 488 and goat anti-rabbit Alexa Fluor 594 (1 : 1000; Jackson ImmunoResearch Laboratories. West Grove, PA). The images were captured using a laser-scanning confocal microscope (Nikon A1, Tokyo, Japan) at 10, 40, or $\times 100$ magnifications and analyzed using the NIS-Elements software (Nikon Instruments, Tokyo, Japan). The images for sagittal sections were captured using a Zeiss Mirax slide scanner at $\times 20$ magnification.

Semi-Quantitative Analysis of FMRP Transfection in the Brain

For a comparative analysis of the transduction pattern in the brain a semi-quantitative scoring system was used to analyze the cellular tropism of the AAV–FMRP in different

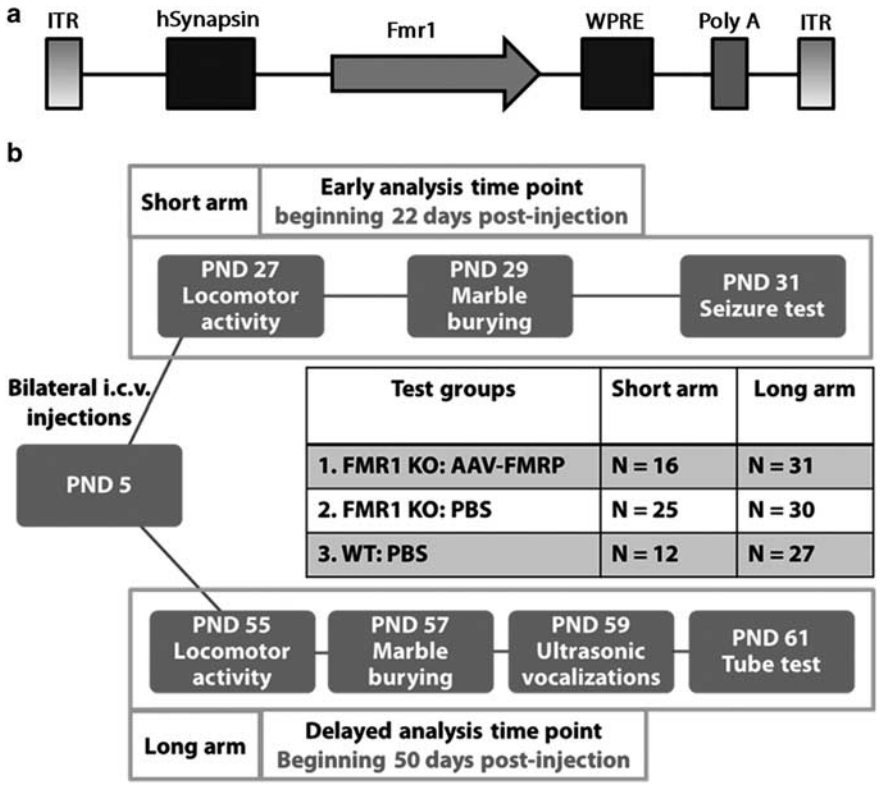

Figure 1 Overview of viral vector construction, experimental plan for injections, and behavioral analyses. (a) Schematic depiction of the AAV–FMRP vector construct. The single-stranded AAV viral vector contained the human SYN promoter and ITR elements from AAV serotype 2 and packaged in serotype 9 capsids. A woodchuck hepatitis post-transcriptional regulatory element was inserted downstream of the mouse Fmr1 cDNA to induce elevation of transcripts. (b) Timelines for the short and long arms of the study for mice injected with PBS or viral vector on PND 5. The total number of mice (*N*) injected for each treatment group is indicated.

Table 1 Quantitative Analysis of AAV–FMRP Transduction in Cingulate Cortex at the end of the Long Arm (PND 61)

Animal #	FMRP + cells/mm^2	NeuN + /FMRP + cells/mm^2	% of neuronal transduction
1	1714 ± 470	1588 ± 403	94 ± 2
2	2154 ± 734	2097 ± 731	96 ± 2
3	2042 ± 666	2003 ± 656	98 ± 1

The cells were counted in three consecutive coronal 25-μm thick sections (100 μm apart) of the cingulate cortex from each brain (total of nine sections from three mice) and reported as the average number of cells per square millimeter ± SEM.

brain regions. Scoring was done by classifying the number of transduced cells in four categories: regions with no detectable FMRP expression, regions with 0–100 FMRP-positive cells/mm^2, regions with 100–200 FMRP-positive cells, and regions with more than 200 FMRP-positive cells. The cingulate cortex was used to calculate the percentage of neuronal transduction. The total number of FMRP-positive cells in each group as well as the percentage of FMRP-positive cells that co-localized with the neuronal marker NeuN in the cingulate cortex were recorded (Table 1).

Quantitative Western Blotting

Samples of the inferior colliculus, cerebellum, cerebral cortex, hippocampus, and striatum were collected and stored at − 80 °C. After electrophoresis, the proteins were transferred onto nitrocellulose membranes and then incubated overnight with primary antibodies including mouse anti-FMRP 5c2 (1 : 250), (LaFauci *et al*, 2013) and mouse anti-GAPDH (1 : 40 000; Clone GAPDH-71.1; Sigma-Aldrich, St Louis, MO). The sections were incubated with HRP-conjugated goat anti-mouse (Jackson ImmunoResearch Laboratories; West Grove, PA); after washing, SuperSignal West Pico Chemiluminescent Substrate (Thermo Scientific; Rockford, IL) was added to the membranes and the bands were revealed by exposure under Alpha Innotec Fluorochem gel imager (Protein Simple; Toronto, ON, Canada). Images were analyzed using AlphaEase SA. Quantification of protein expression was normalized to GAPDH expression. Results are presented as averages ± SEM. Statistical significance was determined by using one-way ANOVA and Tukey's multiple comparison tests.

Behavioral Analyses

All behavioral tests were conducted on aged and sex-matched wild-type and KO animals. All mice were naive to the tests

and tested only once in each test. The experimenters were blinded to the AAV–FMRP and PBS-injected groups during the time of testing.

Locomotor Activity Measurements

Locomotor activity was assessed using an automated open field locomotor monitor system (Accuscan Images, Salt Lake City). Mice were acclimated to the testing room for 5 min, then placed in the open field and monitored for 20 min in the dark. The total distance covered (horizontal movement) was recorded using the Fusion software (Fusion software, Johannesburg, South Africa). Total distance traveled was compared between groups.

Marble Burying for Stereotypic Behavior

Approximately 10 cm of laboratory animal bedding (Bed-o'Cobs combination bedding; Andersons, Maumee) was added to empty cages and blue marbles were placed equidistant from each other in a 4×5 grid covering two thirds of the surface. Mice were acclimated to the testing room for 5 min, and then placed in the cage on the side devoid of marbles. Mouse activity was left undisturbed for 30 min and then the number of buried marbles was counted; a buried marble consisted of any marble where less than 50% of its surface was left uncovered by bedding.

Ultrasonic Vocalizations

Virgin adult female mice were placed in a new cage that contained only bedding for 2 min and the cage was fitted with a customized polystyrene cover. Subsequently, a virgin male was placed into the same cage and ultrasonic vocalizations were recorded using an Ultrasound Detector D 1000X (Pettersson Elektronik AB, Uppsala, Sweden) for 4 min as described previously (Wang *et al*, 2008). The distinct waveform patterns seen in the spectrograph rendering, indicative of vocalizations, were counted. The first 5 s of recording following the introduction of the male was also ignored. The total number of vocalization contained within 4 min of recording was compared between animals.

Tube Test for Social Dominance

The mice were tested using the tube test to measure social dominance. Each match involved two mice of different genotype (wild-type or Fmr1 KO) or injection groups (PBS or AAV–FMRP) that were not housed together. The experimenter was blind to the category of the groups being tested. One mouse was placed into each end of a transparent PVC tube (2.5 cm inner diameter, 30.5 cm length) and the mice were released simultaneously. The match ended when one mouse placed at least two paws outside the tube with the mouse remaining inside the tube being deemed the 'winner'. The number of wins for each group or genotype was tallied and a χ^2 analysis was used to determine whether the percent of wins in each group was significantly different from the 50 : 50 win/loss outcome expected by chance. Each animal was tested three to five times, depending on pairing availability, against animals of opposing injection group and/or genotype.

Audiogenic Seizures

Audiogenic seizure testing was carried out as previously described (Pacey *et al*, 2009). Seizure activity was observed and scored using a severity score as follows: 0, no effect; 1, wild running; 2, clonic seizure; 3, tonic seizure; 4, status epilepticus/respiratory arrest/death. For data analysis, the animals that obtained a score of 0 or 1 were classified as 'no seizures', whereas animals with a score of 2 or more were considered to have experienced seizures. All mice were immediately euthanized at the end of the test.

Statistical Analyses

Fisher's exact test was used for statistical analysis of audiogenic seizure incidence between the groups. In the tube test, a χ^2 analysis was used to determine whether the percent of wins were significantly different from the 50 : 50 win/loss outcome expected by chance. For motor activity test, marble burying test and ultrasonic vocalization tests, one-way ANOVA test was performed followed by Bonferroni *post hoc* test. The GraphPad prism software (version 6) was used to perform the statistical analyses.

RESULTS

Because FMRP is widely distributed throughout most regions of the CNS, a major goal of this study was to identify conditions for AAV–FMRP administration that would provide widespread transgene dispersion in the brain. We also sought to attain a level of expression that was as close to wild-type levels as possible. All analytical assessments were carried out during two periods post injection: the first began 22 days post injection (on PND 27) and is hereafter referred to as the 'short arm', and the second began 50 days post injection (on PND 55) and is referred to as the 'long arm' (see Figure 1b).

Quantification of FMRP Expression Levels Following Neonatal Administration of AAV–FMRP

To quantify total transgene expression, samples of the cerebellum, inferior colliculus, cerebral cortex, striatum, and hippocampus were subjected to quantitative western blotting. In samples from wild-type mice, three bands corresponding to FMRP isoforms were detected (Figure 2). In Fmr1 KO mice injected with AAV–FMRP, as expected, only isoform 1 was observed (Figure 2). Quantitative western blot analysis conducted on brain regions of Fmr1 KO mice injected with AAV–FMRP and killed at PND 31 (Figure 2a and c), revealed $52 \pm 9\%$ of wild-type FMRP expression in the hippocampus, $41 \pm 13\%$ in the striatum, and $71 \pm 20\%$ in the cerebral cortex (Figure 2c). At PND 60 (Figure 2b and c), the AAV–FMRP-injected Fmr1 mice displayed a mean $47 \pm 15\%$ of wild-type expression in the cerebral cortex, $48 \pm 20\%$ of wild-type expression in the hippocampus and $18 \pm 5\%$ of wild-type expression in the striatum (Figure 2c). The results shown in the western blots in Figure 2a, b, and d, and in the error bars shown in the summary graph in Figure 2c clearly reveal variable expression of the transgene from mouse-to-mouse in the brain regions examined. The range of FMRP transgene expression levels in forebrain

regions is likely the result of the ability of the vector to diffuse from the site of the injection in the lateral ventricles. FMRP was not detected in brain regions more distal from the lateral ventricles such as the inferior colliculus and the cerebellum; these brain regions are likely located too far from the ventricles to acquire sufficient vector uptake for transgene expression and detection. Importantly, transgene expression levels in the brain regions where it was detected remained relatively constant for at least 7 months post injection, showing 77 ± 28% of wild-type expression in the cortex, 40 ± 14% in the hippocampus, and 14 ± 3% in the striatum (Figure 2c and d).

Distribution and Cellular Selectivity of Transgene Expression

Immunocytochemical analysis revealed expression of the FMRP transgene in the striatum, hippocampus, retrosplenial cortex, and cingulate cortex at both the end of the short arm (26 days post injection) and the long arm (56–62 days post injection) of the study (Figures 3a and 4). Representative sagittal images of FMRP expression from PBS-injected wild-type and KO mice and AAV–FMRP-injected KO mice are shown in Figure 3b. No FMRP expression was detected in regions more distal and caudal to the site of injection in the lateral ventricles including the piriform cortex, cerebellum, inferior colliculus, and brainstem. The highest transduction efficiencies were observed in the retrosplenial cortex and the cingulate cortex, whereas lower FMRP expression was observed in the striatum (Figures 3a, b and 4).

Double-labeling experiments showed that FMRP was predominantly observed in NeuN-positive cells within the striatum, hippocampus, retrosplenial cortex, and cingulate cortex, suggesting strong preferential expression in neuronal populations (Figures 3c and 4, and Table 1). Quantitative analysis of FMRP-positive cells co-expressing NeuN in the cingulate cortex revealed over 90% neuronal transduc-

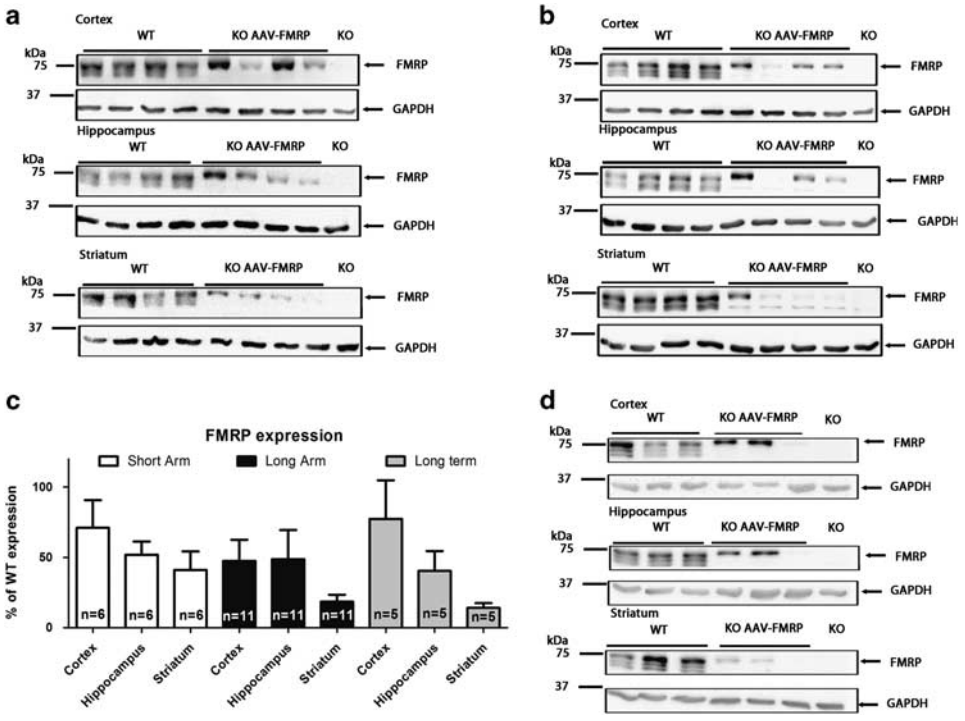

Figure 2 Western blots of FMRP expression in control and AAV–FMRP-treated mice. (a) Representative western blots of the cerebral cortex, hippocampus, and striatum from individual mice injected with AAV–FMRP in the short arm where brain samples were collected at PND 31. (b) FMRP transgene expression in the long arms of the study at PND 60. (c) Quantification of samples from the short and long arms of the study as well as long-term (7 months) expression. Expression in injected Fmr1 KO mice was normalized to the GAPDH signal intensity and compared with age- and sex-matched PBS-injected wild-type brain regions (100% FMRP expression). The results are presented as the mean ± SEM. (d) Representative western blots of Fmr1 KO mice 7 months after i.c.v. injection with AAV–FMRP.

Figure 3 Immunocytochemical analysis of AAV–FMRP transduction in discrete brain regions. (a) Diagrammatic representation of FMRP transgene expression in Fmr1 KO mice treated with AAV–FMRP. The levels of transduction were graded as indicated. (b) Representative low magnification (top row) and higher magnification (bottom row) sagittal images showing FMRP expression in PBS-injected wild-type, AAV–FMRP-injected Fmr1 KO mouse, and PBS-injected Fmr1 KO mouse brain. (c) Photomicrographs depicting neuronal specificity of the AAV–FMRP transductions in the cingulate cortex of mice collected at PND 61. Brain sections were double labeled using anti-FMRP antibody and either the neuronal marker NeuN or the glial specific marker S100β. Scale bars, 20 μm (top row), 50 μm (bottom row). (d) Higher magnification photomicrographs illustrating similar cytosolic distributions of FMRP in the cortex of wild-type and AAV–FMRP-injected KO mice. Scale bars, 20 μm in all panels.

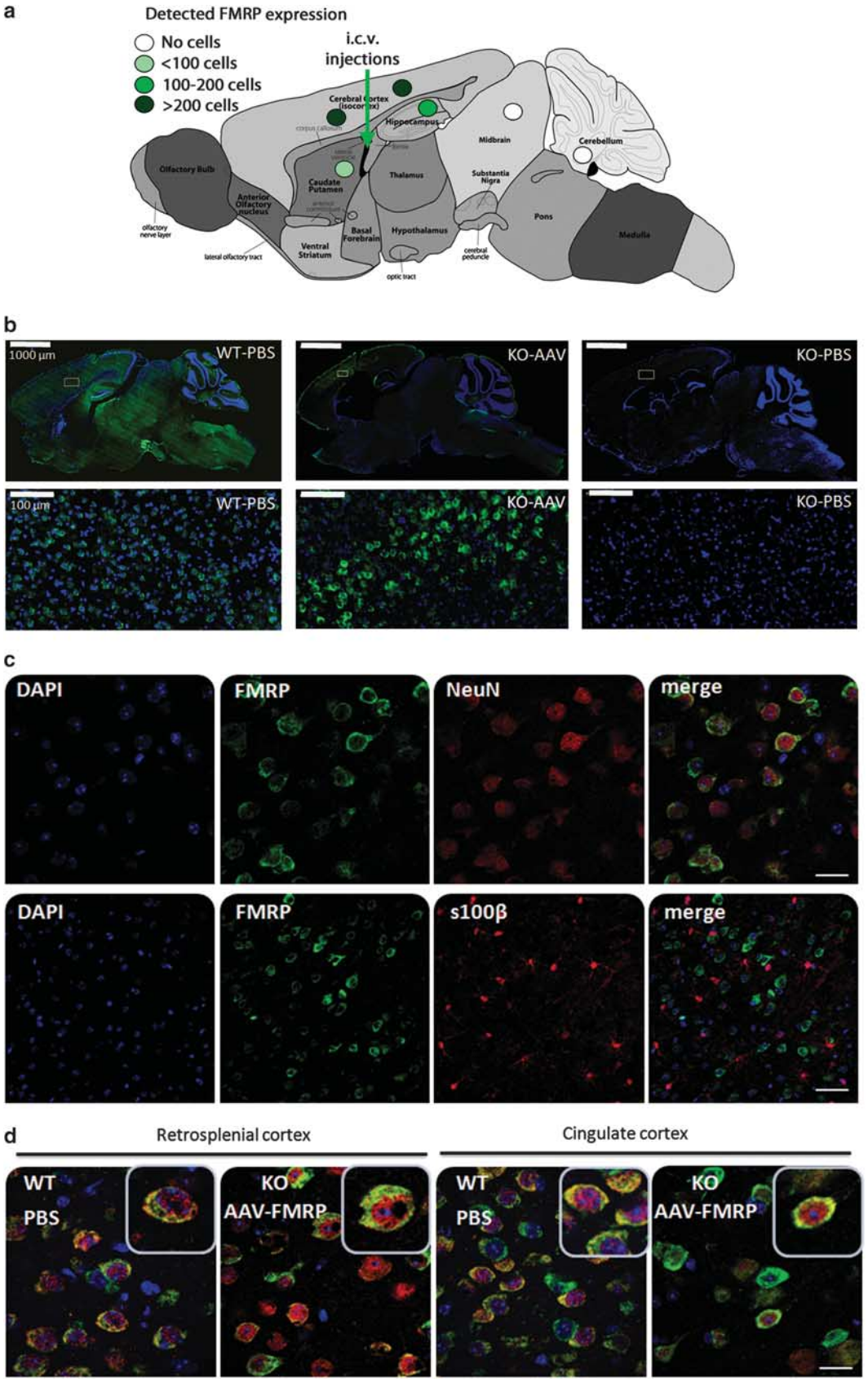
a
Detected FMRP expression
No cells
<100 cells
100-200 cells
>200 cells
i.c.v.
injections
Cerebral Cortex
Hippocampus
Midbrain
Cerebellum
Olfactory Bulb
Caudate
Putamen
Thalamus
Substantia
Nigra
Anterior
Olfactory
nucleus
Basal
Forebrain
Hypothalamus
Pons
Medulla
Ventral
Striatum
b
1000 µm
WT-PBS
KO-AAV
KO-PBS
100 µm
WT-PBS
KO-AAV
KO-PBS
c
DAPI
FMRP
NeuN
merge
DAPI
FMRP
s100β
merge
d
Retrosplenial cortex
Cingulate cortex
WT
PBS
KO
AAV-FMRP
WT
PBS
KO
AAV-FMRP

tion (Table 1). In contrast, we did not detect transduced cells that were immunopositive for the glial selective marker S100β in any of the brain regions examined (Figure 3c), suggesting no or undetectable levels of FMRP transduction in astrocytes. The latter observation is consistent with the use of the neuron-selective synapsin promoter used to drive transgene expression. Analysis of the cellular localization of FMRP in AAV–FMRP transduced cells revealed predominant expression in the cytoplasm of neurons (Figures 3c,d and 4). This cytoplasmic localization of the FMRP transgene was observed in all brain regions where transgene expression was detected and was similar to that observed previously in neurons of wild-type mice (Pacey *et al*, 2013; Devys *et al*, 1993).

Behavioral Analyses

Behavioral experiments were carried out to determine if AAV-induced restoration of FMRP in the brains of Fmr1 mice could rescue or ameliorate pathological behaviors typically seen in Fmr1 KO mice (and observed here in PBS-injected Fmr1 KO mice). In the behavioral tests, if a mouse displayed an obvious abnormality that could influence the test, such as weight loss following malocclusion, it was excluded from the analysis. Overall, this happened infrequently and did not appear to be restricted to any particular treatment group. Additional contributions to the variable number of mice analyzed in each test include the assessment of only male mice in the ultrasonic vocalization

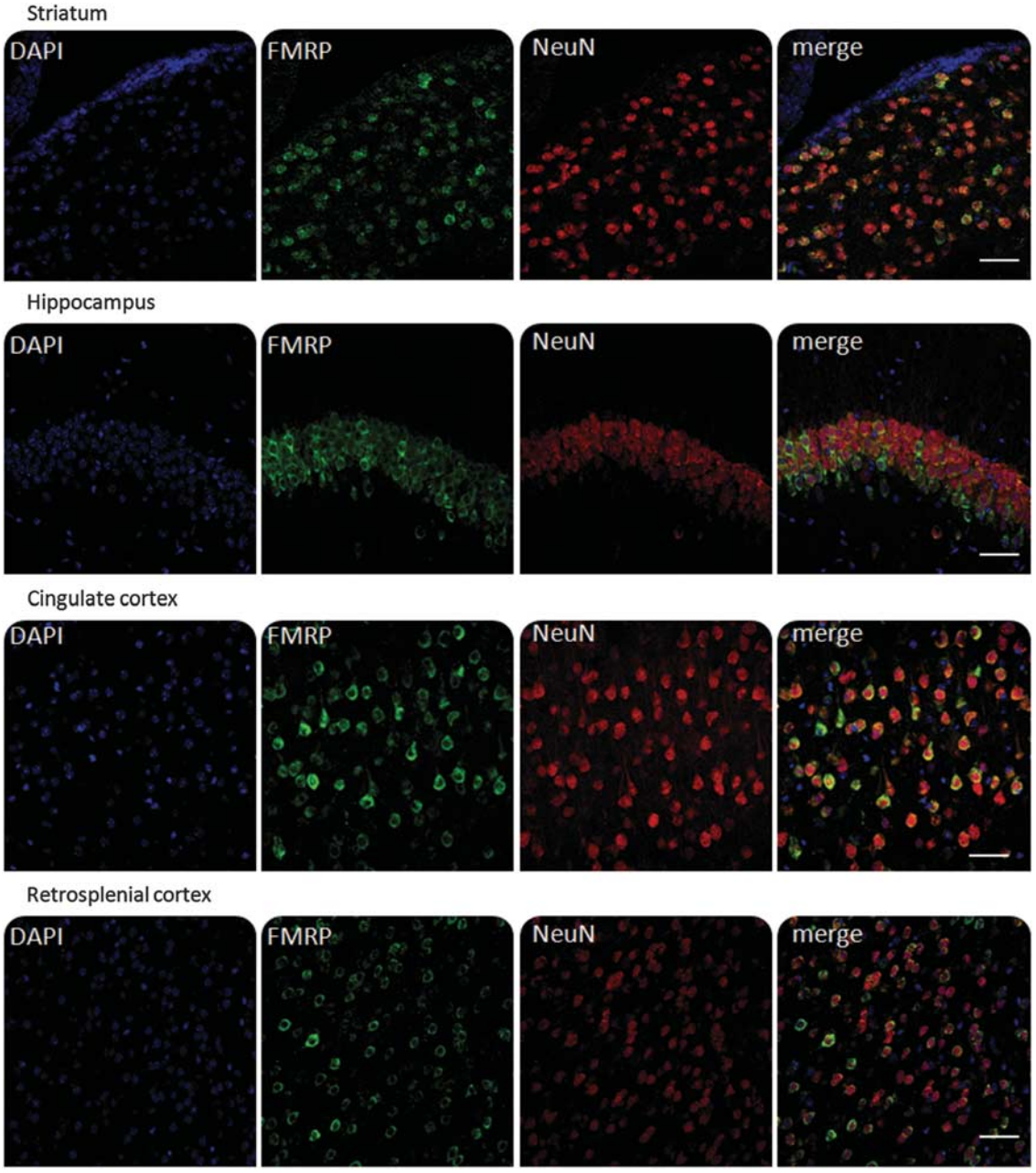

Figure 4 FMRP transgene expression in the striatum, hippocampus, cingulate cortex, and retrosplenial cortex 61 days after i.c.v. administration of AAV–FMRP on PND 5. Brain sections were double labeled using anti-FMRP (green) and anti-NeuN (red). Scale bars = 50 μm.

analysis, and in tube test, the *N* values represent the total number of pairings; this depended on the availability of age-matched groups at the time of testing.

In the short arm of the study, the tests included measurement of locomotor activity, marble burying (as a measure of repetitive behavior), and audiogenic seizure susceptibility. Separate groups of mice were examined in the long arm of the study (ie, no mice studied in the short arm were again studied in the long arm). In the long arm, motor activity and marble burying were measured along with two additional tests: ultrasonic vocalizations to examine mouse-to-mouse communication during courtship behavior, and the tube test, which measures social dominance. In both, the short and long arms, preliminary statistical analyses were conducted using two-way ANOVA on males and females (ie, gender and treatment as the main effects). These results indicated no significant interaction effect between males *vs* females; therefore, further statistical analyses were carried out on pooled data from both males and females.

In the motor activity test, a significant increase in the total distance traveled was seen in both PBS-injected and AAV–FMRP-injected Fmr1 KO mice compared with age and gender-matched PBS-injected wild-type mice in the short and long arms of the study (Figure 5a and Supplementary Figure 1a). Thus, AAV–FMRP vector administration did not rescue the motor hyperactivity in Fmr1 KO mice.

In the marble burying test used as a measure of repetitive behavior, a significant increase was observed in the number of marbles buried by PBS-injected Fmr1 KO mice compared

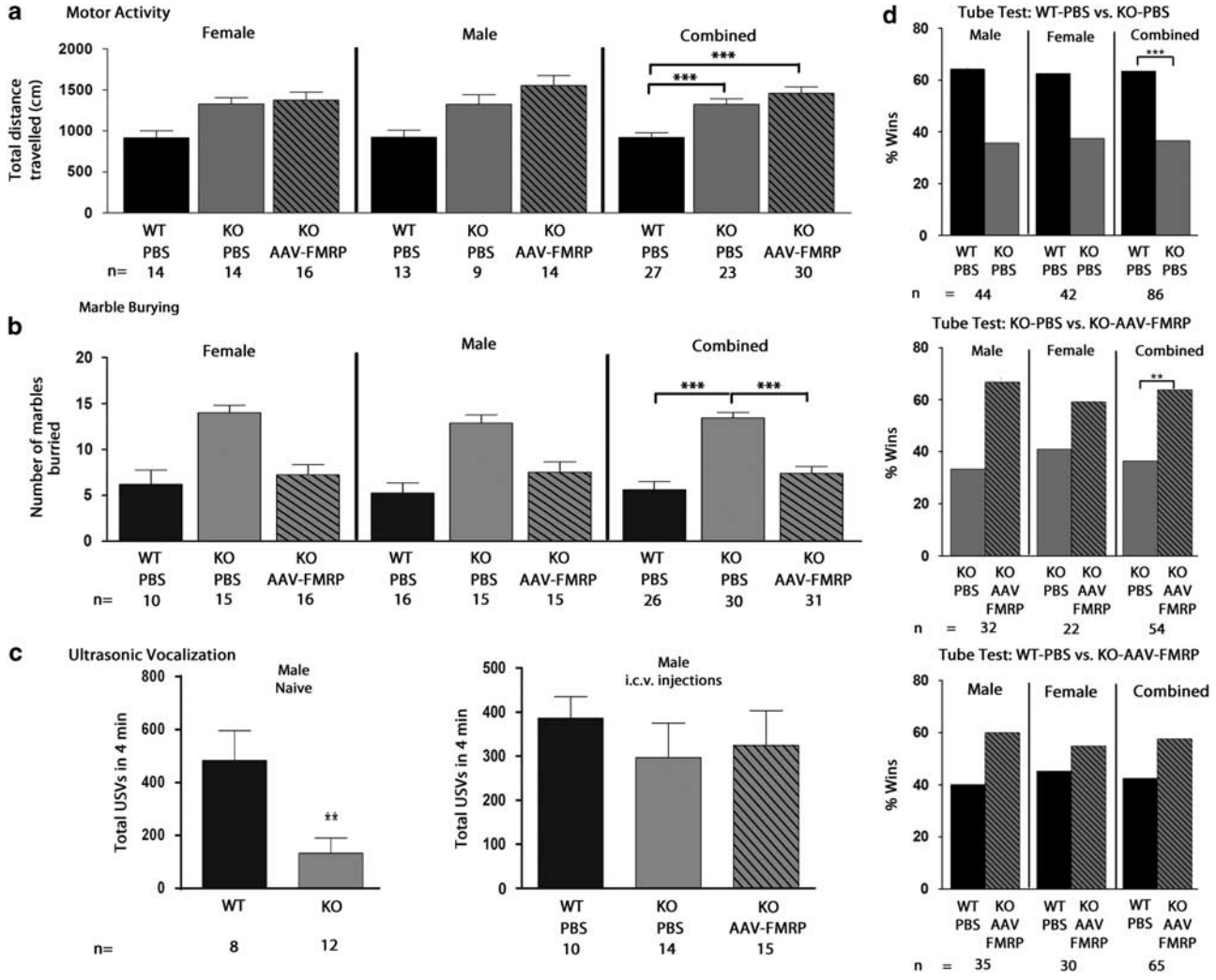

Figure 5 Summary of the behavioral results from the long arm of the study at PNDs 55 to 61. PBS-injected Fmr1 KO mice exhibited hyperactivity, increased repetitive behavior, decreased ultrasonic vocalizations, and a reduction in social dominance behavior compared with PBS-injected wild-type mice. (a) Total horizontal activity over 20 min. (b) Rescue of stereotypical behavior as seen by total number of marbles buried during 30 min. (c) Total number of ultrasonic vocalization calls during a 4-min encounter in naive (left) and treated mice (right). (a–c) Each bar represents the average ± SEM (**$p<0.01$, ***$p<0.001$). (d) Rescue of impaired social dominance in the tube test in AAV–FMRP–Fmr1 KO mice compared with PBS-injected Fmr1 KO mice. Columns indicate total % of wins for each group. The tube test was administered to PBS-treated wild-type paired with PBS–Fmr1 KO mice (top), PBS-treated Fmr1 KO mice paired with AAV–FMRP-treated Fmr1 KO mice (middle), and wild-type PBS paired with AAV–FMRP mice (bottom). The number of wins for each group was tallied and a χ^2 analysis was used to determine whether the scores were significantly different from the 50 : 50 win/loss outcome expected by chance. *n* = the number of pairings. **$p<0.01$, ***$p<0.001$.

with PBS-injected wild-type mice (Figure 5b; $F=29.79$, $p<0.001$), similar to previous observations made in some strains of the Fmr1 KO mouse (Spencer *et al*, 2011). There was a significant decrease in the number of buried marbles in Fmr1 mice injected with AAV–FMRP compared with PBS-injected Fmr1 KO mice (Figure 5b), indicating that the reintroduction of FMRP rescued stereotypical behavior. In the short arm of the study, this trend was also observed but did not reach statistical significance, perhaps due to the lower number of marbles buried by mice in all groups at PND 32 (Supplementary Figure 1b; $F=4.01$, $p>0.05$). To summarize, the trend toward reversal of elevated repetitive behavior seen in the short arm was more robust and statistically significant in the long arm of the study.

For the analysis of audiogenic seizure susceptibility, as expected from previous observations in our laboratory (Pacey *et al*, 2009; Pacey *et al*, 2011b), wild-type C57/BL6J mice were not susceptible to audiogenic seizures. In PBS-injected Fmr1 KO mice, 36% of the females and 31% of the males had seizures. In the combined male plus female data, the incidence of audiogenic seizures in both PBS-injected Fmr1 KO mice and AAV-FMRP-injected mice was significantly elevated compared to PBS-injected wild-type mice (Supplementary Figure 1c; $p<0.05$). However, the AAV–FMRP group was not different than the PBS-injected Fmr1 group.

Ultrasonic vocalizations were recorded from PND 59 male mice. In a preliminary experiment, we tested adult naïve noninjected wild-type and Fmr1 KO and observed a significant decrease in the number of ultrasonic vocalized calls in Fmr1 KO mice compared with wild-type mice (Figure 5c left panel; $F=2.53$, $p<0.01$). This result confirmed a previous finding showing reduced vocalizations in Fmr1 mice (Rotschafer *et al*, 2012). We then conducted a second study comparing male PBS-injected wild-type mice with male PBS-injected and AAV–FMRP-injected Fmr1 mice. Although the number of ultrasonic vocalizations was lower in the PBS–Fmr1 KO group compared with AAV–FMRP–Fmr1 KOs and PBS-treated wild-type mice, there was no statistically significant difference among the three groups (Figure 5c, right panel; $F=0.32$, $p>0.05$).

Impaired social dominance is an established characteristic of Fmr1 KO mice (Pacey *et al*, 2011a; Spencer *et al*, 2005). The tube test measures social dominance and aggressive tendencies without allowing mice to injure one another. Dominant versus submissive behaviors are scored for two age- and sex-matched mice during a brief pairing. For each trial, the more dominant mouse pushes the other more submissive mouse out of the tube and is deemed the winner, whereas the second (subordinate) mouse is the loser. All combinations of wild-type PBS, Fmr1-PBS and Fmr1-AAV-FMRP were evaluated and tallied as the percent of wins by each group against their opponents. As expected, based on previous studies (Pacey *et al*, 2011a; Spencer *et al*, 2005), Fmr1 KO mice injected with PBS won significantly fewer matches than expected by chance against wild-type mice injected with PBS (Figure 5d; $p<0.001$). Male and female Fmr1 animals injected with AAV–FMRP won significantly more matches against gender-matched PBS-injected Fmr1 KO mice (Figure 5d, $p<0.01$). Thus, the deficit in social dominance in Fmr1 KO mice was rescued in the AAV–FMRP-treated mice.

DISCUSSION

FMRP is widely distributed in most neurons throughout the adult mammalian CNS. This wide dispersion throughout the CNS presents a challenge from the perspective of virally mediated gene therapy in terms of achieving sufficiently wide distribution of the viral vector. Of the various AAV vectors currently available, we chose to use AAV9 because of its documented propensity to cross the blood–brain barrier and neuronal tropism (Nonnenmacher and Weber, 2012; Rothermel *et al*, 2013). Other groups investigating approaches for treating CNS disorders in animal models have reported success after direct CNS injections (Daily *et al*, 2011; Gadalla *et al*, 2012), and after intravenous injection of AAV vectors in the mouse (Garg *et al*, 2013) and monkey (Samaranch *et al*, 2012).

However, we chose i.c.v. administration into the lateral ventricles for several reasons including (a) the desire to avoid possible off-target tissue effects such as the liver, a known AAV-targeted organ, (b) to minimize the amount of vector given to the animal, and (c) to specifically scrutinize the effects of FMRP restoration in the brain. The results of our previous work indicated substantial diffusion of a vector coding for eGFP from the ventricles and transgene expression in multiple forebrain regions of the mouse CNS (Gholizadeh *et al*, 2013). Relevant conclusions gleaned from that AAV9–eGFP study were that the age of injection and the promoter employed were critical factors in determining the distribution and cell type transduction specificity of the transgene. We speculate that one parameter that may promote the spread of the viral vector in the brain after i.c.v. administration is the recently characterized 'glymphatic system'. Similar in function to the peripheral lymphatic system, in brain parenchyma, perivascular exchange between cerebrospinal fluid and interstitial fluid has been shown to be facilitated by astroglial water transport mediated in part by the aquaporin-4 water channel (Iliff *et al*, 2013).

In the adult mammalian CNS, FMRP is highly expressed in neurons (Cruz-Martín *et al*, 2010; Harlow *et al*, 2010). In the present study, double-labeling immunocytochemical analysis demonstrated that AAV–FMRP transduction occurred primarily in neurons rather than glia, as expected from the incorporation of the neuron-selective synapsin promoter in the AAV–FMRP vector construct. Analysis of the anatomical distribution of the recombinant FMRP transgene in AAV–FMRP-treated Fmr1 KO mice indicated that it was present in several forebrain regions including the retrosplenial and cingulate cortices, the hippocampus, and the striatum. FMRP was not detected in brain regions located more distal from the lateral ventricles such as the piriform cortex, inferior colliculus, cerebellum, and brainstem. The presence of the FMRP transgene in the observed brain regions (cerebral cortex, hippocampus, and striatum), and its absence in other regions provided an opportunity to link the restoration of FMRP expression in specific brain regions to corrected pathological behaviors observed in PBS-injected Fmr1 KO mice. Our data suggest that the presence of FMRP in the cortex and/or the striatum of the AAV–FMRP-treated mice could have been responsible for the reduction in repetitive behavior as assessed by the marble burying test. Several lines of evidence have shown that lesions of the dorsal or ventral striatum in rodents

(Aliane *et al*, 2011) and non-human primates (Saka *et al*, 2004) block stereotyped behavior. Moreover, in a longitudinal study of brain development in children, it was shown that an increased growth rate of the striatum was correlated with more severe repetitive behavior in autistic children compared with control subjects (Langen *et al*, 2013).

Our results suggest that high levels of FMRP transgene expression in neurons of the cingulate cortex might be responsible for the rescue of social dominance observed in the tube test. The medial prefrontal cortex, which includes the cingulate cortex, subcallosal cortex, and the medial frontal gyrus, has been shown to be linked with social dominance in mice. Based on recordings from pyramidal neurons of the medial prefrontal cortex, Wang *et al*, 2011 reported that social rank in mice directly correlates with the synaptic strength of pyramidal neurons in the medial prefrontal cortex (Wang *et al*, 2011). It has also been reported that levels of proteins involved in synaptic function, including the NMDA receptor subunits NR1, NR2A, and NR2B, are decreased in the medial prefrontal cortex of Fmr1 KO mice (Krueger *et al*, 2011).

In contrast to the correction of abnormal repetitive behavior and social dominance, we did not observe reversal of other pathological behaviors including motor hyperactivity, ultrasonic vocalizations, and audiogenic seizures. There are several potential, non-mutually exclusive explanations for the lack of full reversal of all the abnormal phenotypes examined. First, it is conceivable that the lack of expression of the FMRP transgene (containing a neuron-selective promoter) in glial cell populations may have been a contributing factor. Second, the expression of only one of the several known isoforms of the protein present in the CNS could have been responsible for the lack of full phenotypic reversal. However, we expressed FMRP isoform 1 because it is widely expressed in most brain regions and is one of the more abundant forms of FMRP in the mouse brain (Brackett *et al*, 2013; Dury *et al*, 2013).

Another potential explanation for the lack of full behavioral recovery is the apparent absence of diffusion of the viral vector from the lateral ventricles to more distal regions of the CNS. We believe that this may be one of the more crucial factors contributing to the inability, under the conditions used, to achieve a complete rescue of all the aberrant behaviors assessed. Several brain regions where no FMRP transgene was detected are thought to be linked to behaviors associated with FXS. For example, FMRP is present in all neuronal populations of the cerebellum (Pacey *et al*, 2013) and the cerebellum has been consistently associated with neuropathology in FXS (Ellegood *et al*, 2010; Fatemi *et al*, 2012) and autism (Whitney *et al*, 2008). The cerebellum has also been linked with motor hyperactivity in Fmr1 KO mice (Rogers *et al*, 2013). The absence of FMRP in the inferior colliculus and the brainstem of the AAV–FMRP-treated Fmr1 KO mice might explain the lack of reversal or amelioration of audiogenic seizure susceptibility. These brain regions have been linked to auditory processing and are thought to be important for propagation of auditory seizures (Chen and Toth, 2001; Yang *et al*, 2001).

The results presented here provide a proof of principle demonstrating that expression of recombinant FMRP in specific regions of the CNS of the Fmr1 KO mouse are capable of reversing selected neurological abnormalities in this widely used animal model of FXS. The exceptionally protracted expression of AAV-mediated transgenes as shown here (at least 7 months post transfection), and in other studies using AAV transduction in the brain (up to 1 year post injection; Mattar *et al*, 2012; Miyake *et al*, 2011), makes this approach especially attractive for treating neurodevelopmental disorders where the presence of the missing protein is likely required over an extended time frame.

The variable level of FMRP transgene expression in AAV–FMRP-injected animals could provide an opportunity to examine potential correlations between FMRP expression and behavioral rescue. Our current data set is too small for an extensive examination of this issue in the present study. Nevertheless, a preliminary analysis based on a small set of data points, suggests a possible inverse correlation whereby the level of repetitive behaviors in the marble burying test goes up as FMRP expression go down ($r^2 = 0.37$, $p = 0.06$; Supplementary Figure 2). Although no other trends were seen in our current data set with wild-type or AAV–FMRP-injected mice, a more in-depth analysis of such correlations will be a priority in our future studies. Further investigation of other parameters affecting the outcome of AAV-mediated gene therapy is also required to optimize conditions for obtaining a complete reversal of this disorder. These parameters include further exploration of the routes and timing of AAV administration, an examination of other AAV serotypes, and testing additional variations in AAV vector construction that alter cell type selectivity and the level of expression.

FUNDING AND DISCLOSURE

The authors declare no conflict of interest.

ACKNOWLEDGEMENTS

We thank Drs Jennifer Darnell (Rockefeller University) and Richard Kascsak (New York State Institute for Basic Research in Developmental Disabilities) for antibodies, Shu-Jen Chen and Arbansjit Sandhu at the University of Pennsylvania for advice on AAV, and Amy Ramsey and John Yeoman at the University of Toronto for use of equipment. This work was supported by grants from the Fragile X Research Foundation of Canada and the Canadian Institutes of Health Research. SG was supported by a Vanier Canada Graduate Scholarship and JA and ICYX were supported by the CIHR Biological Therapeutics Training Program.

REFERENCES

Aliane V, Perez S, Bohren Y, Deniau JM, Kemel ML (2011). Key role of striatal cholinergic interneurons in processes leading to arrest of motor stereotypies. *Brain* **134**(Pt 1): 110–118.

Ascano M, Mukherjee N, Bandaru P, Miller JB, Nusbaum JD, Corcoran DL *et al* (2012). FMRP targets distinct mRNA sequence elements to regulate protein expression. *Nature* **492**: 382–386.

Bagni C, Tassone F, Neri G, Hagerman R (2012). Fragile X syndrome: causes, diagnosis, mechanisms, and therapeutics. *J Clin Investig* **122**: 4314–4322.

Brackett DM, Qing F, Amieux PS, Sellers DL, Horner PJ, Morris DR (2013). FMR1 transcript isoforms: association with

polyribosomes; regional and developmental expression in mouse brain. *PloS One* **8**: e58296.

Castren E, Elgersma Y, Maffei L, Hagerman R (2012). Treatment of neurodevelopmental disorders in adulthood. *J Neurosci* **32**: 14074–14079.

Chen L, Toth M (2001). Fragile X mice develop sensory hyperreactivity to auditory stimuli. *Neuroscience* **103**: 1043–1050.

Colak D, Zaninovic N, Cohen MS, Rosenwaks Z, Yang WY, Gerhardt J *et al* (2014). Promoter-bound trinucleotide repeat mRNA drives epigenetic silencing in fragile X syndrome. *Science* **343**: 1002–1005.

Cruz-Martín A, Crespo M, Portera-Cailliau C (2010). Delayed stabilization of dendritic spines in fragile X mice. *J Neurosci* **30**: 7793–7803.

Daily J, Nash K, Jinwal U, Golde T, Rogers J, Peters M *et al* (2011). Adeno-associated virus-mediated rescue of the cognitive defects in a mouse model for Angelman syndrome. *PloS One* **6**: e27221.

Darnell J, Van Driesche S, Zhang C, Hung K, Mele A, Fraser C *et al* (2011). FMRP stalls ribosomal translocation on mRNAs linked to synaptic function and autism. *Cell* **146**: 247–261.

Devys D, Lutz Y, Rouyer N, Bellocq JP, Mandel JL (1993). The FMR-1 protein is cytoplasmic, most abundant in neurons and appears normal in carriers of a fragile X premutation. *Nat Genet* **4**: 335–340.

Dölen G, Osterweil E, Rao BS, Smith G, Auerbach B, Chattarji S *et al* (2007). Correction of fragile X syndrome in mice. *Neuron* **56**: 955–962.

Dury AY, El Fatimy R, Tremblay S, Rose TM, Cote J, De Koninck P *et al* (2013). Nuclear fragile X mental retardation protein is localized to Cajal bodies. *PLoS Genet* **9**: e1003890.

Ellegood J, Pacey L, Hampson D, Lerch J, Henkelman R (2010). Anatomical phenotyping in a mouse model of fragile X syndrome with magnetic resonance imaging. *NeuroImage* **53**: 1023–1029.

Fatemi SH, Aldinger KA, Ashwood P, Bauman ML, Blaha CD, Blatt GJ *et al* (2012). Consensus paper: pathological role of the cerebellum in autism. *Cerebellum* **11**: 777–807.

Fatemi SH, Folsom TD (2011). The role of fragile X mental retardation protein in major mental disorders. *Neuropharmacology* **60**: 1221–1226.

Gabel LA, Won S, Kawai H, McKinney M, Tartakoff AM, Fallon JR (2004). Visual experience regulates transient expression and dendritic localization of fragile X mental retardation protein. *J Neurosci* **24**: 10579–10583.

Gadalla K, Bailey M, Spike R, Ross P, Woodard K, Kalburgi S *et al* (2012). Improved survival and reduced phenotypic severity following AAV9/MECP2 gene transfer to neonatal and juvenile male Mecp2 knockout mice. *Mol Ther* **21**: 18–30.

Garg S, Lioy D, Cheval H, McGann J, Bissonnette J, Murtha M *et al* (2013). Systemic delivery of MeCP2 rescues behavioral and cellular deficits in female mouse models of Rett Syndrome. *J Neurosci* **33**: 13612–13620.

Gholizadeh S, Tharmalingam S, MacAldaz ME, Hampson DR (2013). Transduction of the central nervous system after intracerebroventricular injection of adeno-associated viral vectors in neonatal and juvenile mice. *Hum Gene Ther Methods* **24**: 205–213.

Gray S (2012). Gene therapy and neurodevelopmental disorders. *Neuropharmacology* **68**: 136–142.

Hampson D, Gholizadeh S, Pacey LK (2012). Pathways to drug development for autism spectrum disorders. *Clin Pharmacol Ther* **91**: 189–200.

Harlow EG, Till SM, Russell TA, Wijetunge LS, Kind P, Contractor A (2010). Critical period plasticity is disrupted in the barrel cortex of FMR1 knockout mice. *Neuron* **65**: 385–398.

Iliff JJ, Wang M, Zeppenfeld DM, Venkataraman A, Plog BA, Liao Y *et al* (2013). Cerebral arterial pulsation drives paravascular CSF-interstitial fluid exchange in the murine brain. *J Neurosci* **33**: 18190–18199.

Kim H, Gibboni R, Kirkhart C, Bao S (2013a). Impaired critical period plasticity in primary auditory cortex of fragile X model mice. *J Neurosci* **33**: 15686–15692.

Kim J-Y, Ash R, Ceballos-Diaz C, Levites Y, Golde T, Smirnakis S *et al* (2013b). Viral transduction of the neonatal brain delivers controllable genetic mosaicism for visualising and manipulating neuronal circuits *in vivo*. *Eur J Neurosci* **37**: 1203–1220.

Krueger DD, Osterweil EK, Chen SP, Tye LD, Bear MF (2011). Cognitive dysfunction and prefrontal synaptic abnormalities in a mouse model of fragile X syndrome. *Proc Natl Acad Sci USA* **108**: 2587–2592.

LaFauci G, Adayev T, Kascsak R, Nolin S, Mehta P, Brown WT *et al* (2013). Fragile X screening by quantification of FMRP in dried blood spots by a Luminex immunoassay. *J Mol Diagn* **15**: 508–517.

Langen M, Bos D, Noordermeer SD, Nederveen H, van Engeland H, Durston S (2013). Changes in the development of striatum are involved in repetitive behavior in autism. *Biological Psychiatry* (doi:10.1016/j.biopsych.2013.08.13).

Ludwig AL, Espinal GM, Pretto DI, Jamal AL, Arque G, Tassone F *et al* (2014). CNS expression of murine fragile X protein (FMRP) as a function of CGG-repeat size. *Hum Mol Genet* **23**: 3228–3238.

Mattar C, Waddington S, Biswas A, Johana N, Ng X, Fisk A *et al* (2012). Systemic delivery of scAAV9 in fetal macaques facilitates neuronal transduction of the central and peripheral nervous systems. *Gene Ther* **20**: 69–83.

Miyake N, Miyake K, Yamamoto M, Hirai Y, Shimada T (2011). Global gene transfer into the CNS across the BBB after neonatal systemic delivery of single-stranded AAV vectors. *Brain Res* **1389**: 19–26.

Nonnenmacher M, Weber T (2012). Intracellular transport of recombinant adeno-associated virus vectors. *Gene Ther* **19**: 649–658.

Pacey LK, Doss L, Cifelli C, van der Kooy D, Heximer SP, Hampson DR (2011a). Genetic deletion of regulator of G-protein signaling 4 (RGS4) rescues a subset of fragile X related phenotypes in the FMR1 knockout mouse. *Mol Cell Neurosci* **46**: 563–572.

Pacey LK, Heximer SP, Hampson DR (2009). Increased GABA(B) receptor-mediated signaling reduces the susceptibility of fragile X knockout mice to audiogenic seizures. *Mol Pharmacol* **76**: 18–24.

Pacey LKK, Tharmalingam S, Hampson DR (2011b). Subchronic administration and combination metabotropic glutamate and GABAB receptor drug therapy in fragile X syndrome. *J Pharmacol Exp Ther* **338**: 897–905.

Pacey LKK, Xuan ICY, Guan S, Sussman D, Henkelman RM, Chen Y *et al* (2013). Delayed myelination in a mouse model of fragile X syndrome. *Hum Mol Genet* **22**: 3920–3930.

Pop AS, Gomez-Mancilla B, Neri G, Willemsen R, Gasparini F (2014). Fragile X syndrome: a preclinical review on metabotropic glutamate receptor 5 (mGluR5) antagonists and drug development. *Psychopharmacology (Berl)* **231**: 1217–1226.

Rogers TD, Dickson PE, McKimm E, Heck DH, Goldowitz D, Blaha CD *et al* (2013). Reorganization of circuits underlying cerebellar modulation of prefrontal cortical dopamine in mouse models of autism spectrum disorder. *Cerebellum* **12**: 547–556.

Rothermel M, Brunert D, Zabawa C, Diaz-Quesada M, Wachowiak M (2013). Transgene expression in target-defined neuron populations mediated by retrograde infection with adeno-associated viral vectors. *J Neurosci* **33**: 15195–15206.

Rotschafer SE, Trujillo MS, Dansie LE, Ethell IM, Razak KA (2012). Minocycline treatment reverses ultrasonic vocalization production deficit in a mouse model of Fragile X Syndrome. *Brain Res* **1439**: 7–14.

Saka E, Goodrich C, Harlan P, Madras BK, Graybiel AM (2004). Repetitive behaviors in monkeys are linked to specific striatal activation patterns. *J Neurosci* **24**: 7557–7565.

Samaranch L, Salegio EA, San Sebastian W, Kells AP, Foust KD, Bringas JR *et al* (2012). Adeno-associated virus serotype 9

transduction in the central nervous system of nonhuman primates. *Hum Gene Ther* **23**: 382–389.
Spencer C, Alekseyenko O, Hamilton S, Thomas A, Serysheva E, Yuva-Paylor L *et al* (2011). Modifying behavioral phenotypes in Fmr1KO mice: genetic background differences reveal autistic-like responses. *Autism Res* **4**: 40–56.
Spencer C, Alekseyenko O, Serysheva E, Yuva-Paylor L, Paylor R (2005). Altered anxiety-related and social behaviors in the Fmr1 knockout mouse model of fragile X syndrome. *Genes Brain Behav* **4**: 420–430.
Thomas AM, Bui N, Graham D, Perkins JR, Yuva-Paylor LA, Paylor R (2011). Genetic reduction of group 1 metabotropic glutamate receptors alters select behaviors in a mouse model for fragile X syndrome. *Behav Brain Res* **223**: 310–321.
Wang F, Zhu J, Zhu H, Zhang Q, Lin Z, Hu H (2011). Bidirectional control of social hierarchy by synaptic efficacy in medial prefrontal cortex. *Science* **334**: 693–697.
Wang H, Liang S, Burgdorf J, Wess J, Yeomans J (2008). Ultrasonic vocalizations induced by sex and amphetamine in M2, M4, M5 muscarinic and D2 dopamine receptor knockout mice. *PloS One* **3**: e1893.
Whitney ER, Kemper TL, Bauman ML, Rosene DL, Blatt GJ (2008). Cerebellar Purkinje cells are reduced in a subpopulation of autistic brains: a stereological experiment using calbindin-D28k. *Cerebellum* **7**: 406–416.
Wijetunge LS, Chattarji S, Wyllie DJ, Kind PC (2013). Fragile X syndrome: from targets to treatments. *Neuropharmacology* **68**: 83–96.
Yang L, Long C, Faingold CL (2001). Audiogenic seizure susceptibility is induced by termination of continuous infusion of gamma-aminobutyric acid or an N-methyl-D-aspartic acid antagonist into the inferior colliculus. *Exp Neurol* **171**: 147–152.
Zeier Z, Kumar A, Bodhinathan K, Feller JA, Foster TC, Bloom DC (2009). Fragile X mental retardation protein replacement restores hippocampal synaptic function in a mouse model of fragile X syndrome. *Gene Ther* **16**: 1122–1129.

Supplementary Information accompanies the paper on the Neuropsychopharmacology website (http://www.nature.com/npp)